ACS APPLIED MATERIALS & INTERFACES

Letter

www.acsami.org

Smart Composite Nanosheets with Adaptive Optical Properties

Jeong-Hwan Kim,*[,†] Murtaza Bohra,[†] Vidyadhar Singh,[†] Cathal Cassidy,[†] and Mukhles Sowwan*[,†,§]

[†]Okinawa Institute of Science and Technology, 1919-1 Tancha, Onna-Son, Okinawa 904-0495, Japan

[§]Nanotechnology Research Laboratory, Al-Quds University, East Jerusalem, Palestine

Supporting Information

ABSTRACT: We report efficient design and facile synthesis of size-tunable organic/inorganic nanosheets, via a straightforward liquid exfoliation-adsorption process, of a near percolating gold (Au) thin film deposited onto a branched polyethylenimine (bPEI) matrix. The nanosheets are stiff enough to sustain their two-dimensional (2D) nature in acidic conditions, yet flexible enough to undergo a perfect reversible shape transformation to 1D nanoscrolls in alkaline conditions. The shape transformations, and associated optical property changes, at different protonation states are monitored by transmission electron microscopy (TEM), atomic force microscopy (AFM), UV–visible spectroscopy and zeta potential measurements. Because of their large surface area, both nanosheets and nanoscrolls could be used as capturing substrates for surface-enhanced Raman scattering (SERS) applications.

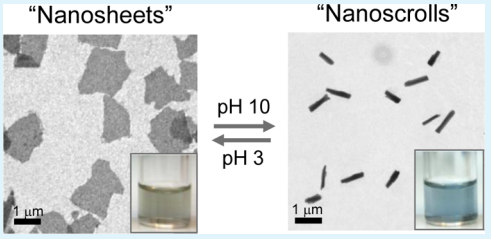

KEYWORDS: *smart materials, nanosheets, nanocomposite, nanoscrolls*

Biological surfaces and interfaces in nature can adapt or respond efficiently to a wide range of external stimuli from the surrounding environment.[1,2] For example, the touch-me-not-plant (*Mimosa pudica*) has leaves that fold inward and bend when touched or shaken. The Venus flytrap (*Dionaea muscipula*) has wide-open leaves with sensitive hair-like sensors on the surface. Once triggered by an insect, the leaves close and trap the insect. Some flowers are sensitive to light or temperature, such as the Moss rose (*Portuclaca grandiflora*), which opens only in bright sunlight and closes at night.[1−5]

Scientists have been trying for the last few decades to learn from such biosystems to design and create smart polymer materials that can mimic such behavior and utilize them in technological applications.[6−12] A specific example is polymer brush technology—a layer of polymer chains with one end attached or grafted onto a thin film surface—which has attracted extensive research studies in the past decade due to its potential application in sensors, actuators and drug delivery systems.[3] The variations in polymer chain conformations in response to external stimuli lead to a transition between shrunk and expanded state. The huge difference between these two states generates large stress and causes strong bending of the surface/brush.[3,13−15] The response mechanism of the brush depends on the polymer type and molecular weight. For example, poly(*N*-isopropylacrylamide) brushes are sensitive to temperature, while triblock poly(styreneblock-2-vinylpyridine-block-ethylene oxide) copolymer brushes are sensitive to pH.[13−15] Despite all these interesting studies and applications, the research in this area is far from maturity. Most of the previously reported systems respond to external stimuli by simple movements such as limited bending, longitudinal shrinkage or expansion.[6,9,10,12] More complicated and controlled movements are required to expand the applications of these systems, especially in the biomedical field.[6,10]

Herein, we report the facile synthesis of size-tunable pH-sensitive Au-bPEI composite nanosheets. These nanosheets undergo controlled, and reversible shape transformation from nanosheets to 1D nanoscrolls in response to variation in the pH value of the surrounding media. bPEI is chosen because it is a smart polymer "proton sponge", which becomes expanded at protonated states (lower pH values) and shrinks at non-protonated states (higher pH values).[16]

To prepare the nanosheets, a sequence of physical deposition, chemical exfoliation, and surface adsorption was developed, as illustrated in Figure 1a-d. The Au nucleation and growth evolves as a function of deposition time, as is characteristic of the different stages of Au-thin film formation on a substrate surface.[17,18] A typical growth sequence for sputtered metal films is initial island formation, elongated island formation, percolation, hole-filling, and finally formation of a continuous thin film.[18] In our case, Au was sputtered onto the bPEI-coated Si substrate until a near-percolating Au thin film was obtained (see Figure S1 in the Supporting Information). The Au-bPEI film was dipped into methanol, exfoliated by ultrasonication, and the suspension was purified to remove the unbound bPEI chains. Finally, the collected nanosheets were resuspended in deionized water. For transmission electron microscopy (TEM) analysis, a small volume of the suspension was placed onto a carbon grid and the water was allowed to evaporate, leaving the nanosheets lying flat on the TEM grid, confirming the 2D nature of the nanosheets (Figure 1e,f). The size of the nanosheets was tunable between hundreds of nanometers and several microns by varying the sonication time

Received: June 27, 2014
Accepted: August 12, 2014
Published: August 12, 2014

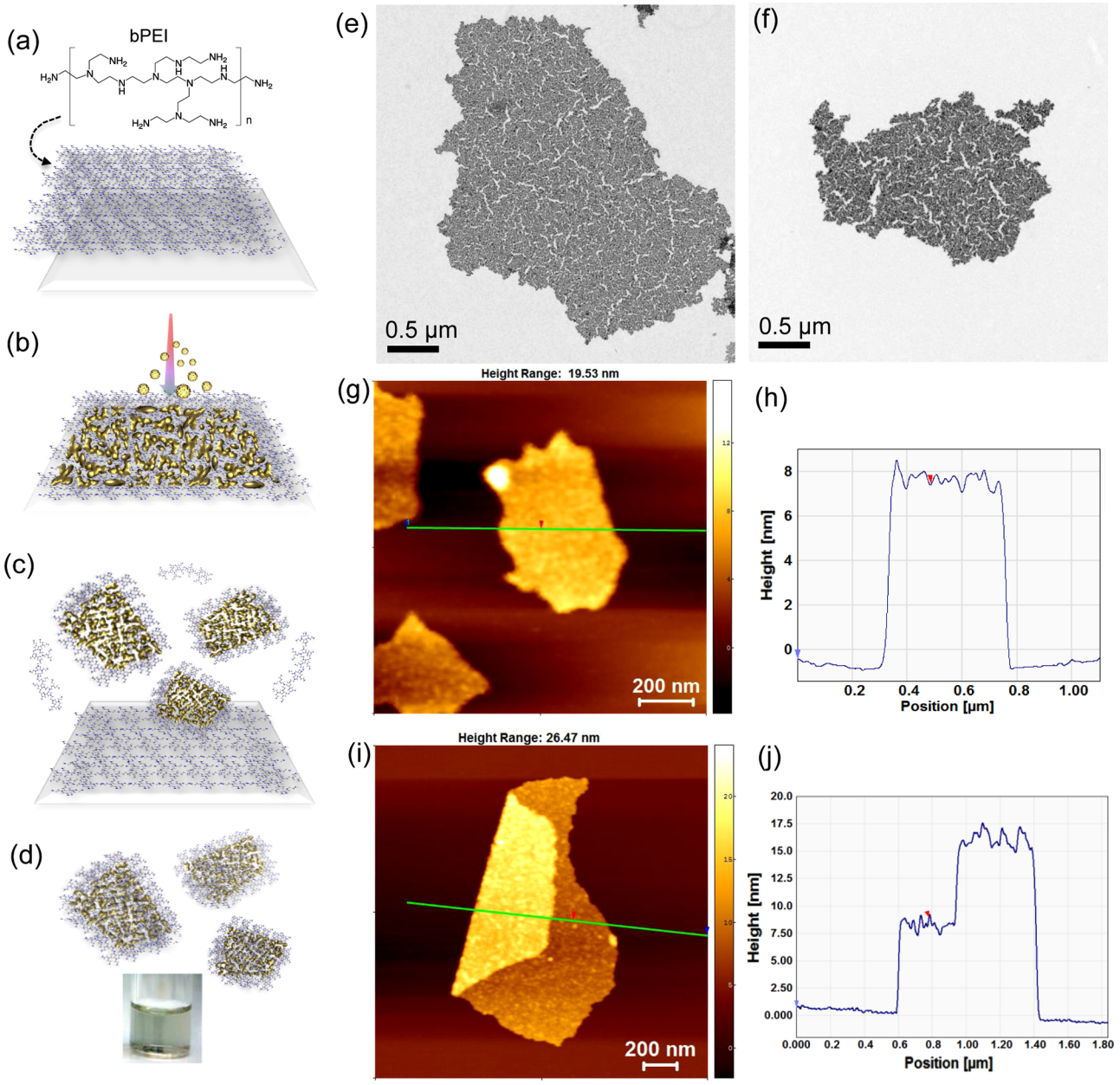

Figure 1. Schematic of the preparation and characterization of bPEI-Au nanosheets. (a) bPEI matrix was spin-coated onto a silicon wafer, (b) Au was sputtered onto the polymer-coated Si until a percolating Au thin film was obtained, forming the Au nanostructure, (c) the sample was dipped in methanol and exfoliated by ultrasonication, (d) purification and resuspension of the nanosheets in deionized water, (e) TEM image of size-tunable exfoliated large nanosheet (prepared at 20 W for 30 min) and (f) small nanosheet (prepared at 20 W for 45 min). (g) Tapping mode AFM topography image of the nanosheets on Si substrate, and (h) cross-sectional height profile showing the thickness of a nanosheet ~8 nm. (i) Tapping mode AFM topography image of a folded precipitated nanosheet, and (j) cross-sectional height profile, clearly showing that the folded region is twice the thickness of the unfolded region.

and power (see Figure S2 in the Supporting Information). Relatively large-sized (5−20 μm) fragments of nanosheets were produced by sonication either at 10 W for 30 min or 20 W for 15 min, whereas the smaller-sized (800 nm to 4 μm) fragments of nanosheets were obtained at >20 W range for >30 min). Occasionally large nanosheets appear to be folded at the edges, as a result of precipitation on the solid support. To measure the thickness, the nanosheets were dispersed on a silicon (Si) substrate and scanned in peak force tapping mode atomic force microscopy (AFM) (Figure 1g, i). The associated cross-sectional height profiles are shown in Figure 1h, j. In this way the average thickness of the nanosheets was determined to be 5.9 ± 0.7 nm from 100 cross-sectional height profiles (see Figure S3 in the Supporting Information).

It is worth noting that varying the thickness of the spin-coated bPEI polymer on the silicon substrate from tens of nanometers to several micrometers did not affect the average thickness of the nanosheets. This is because the polymer is branched (not cross-linked), thus once a single layer of branched polymer has been adsorbed onto the Au nano-domains, there can be no further increase in the thickness of the polymer layer, confirming the validity of the method used to prepare the nanosheets.

dx.doi.org/10.1021/am5041708 | ACS Appl. Mater. Interfaces 2014, 6, 13339−13343

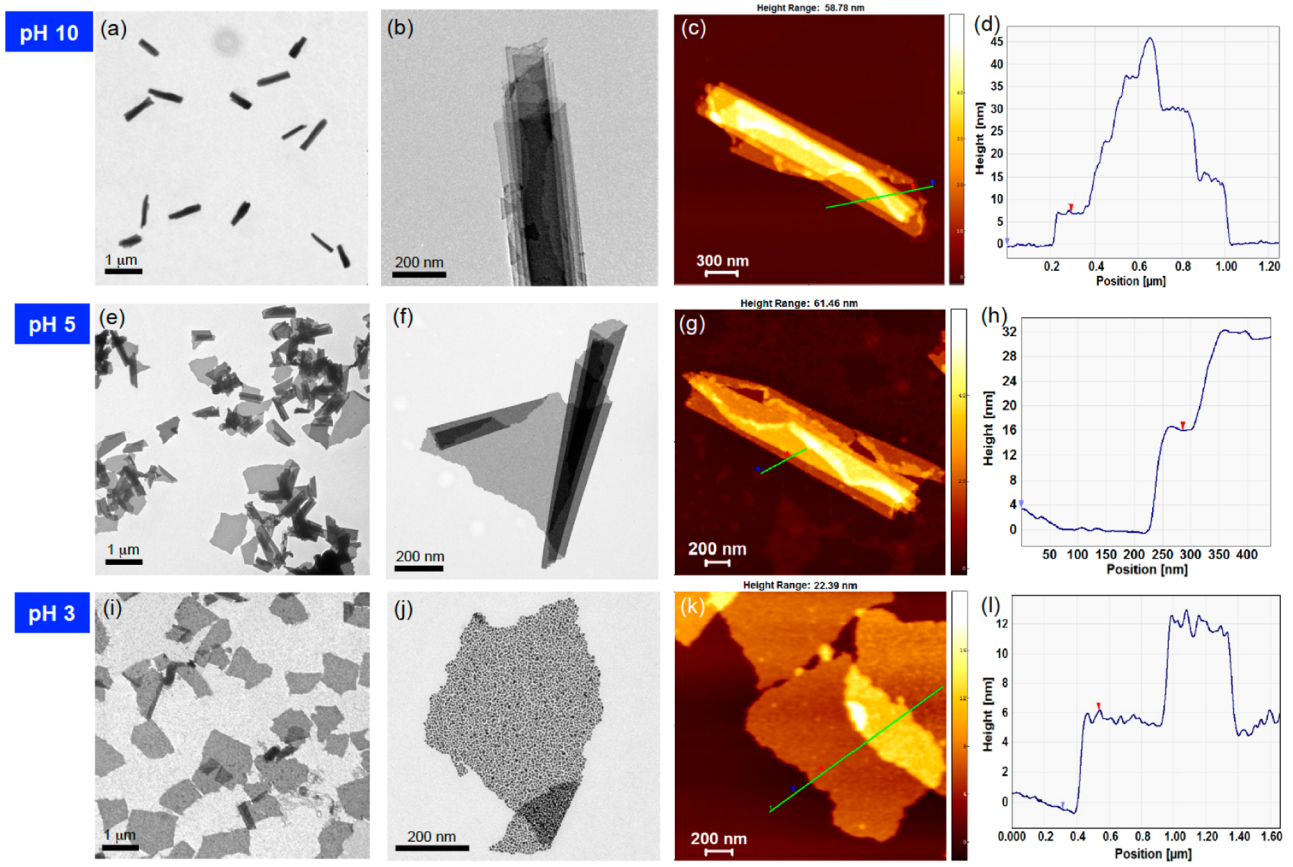

Figure 2. pH-responsive behavior of the nanosheets: (a–d) fully rolled nanosheets at pH 10, (e–h) partially unrolled nanosheets at pH 5, (i–l) unrolled flat nanosheets at pH 3. (a, e, i) Survey TEM showing rolled, partially unrolled, and fully unrolled nanosheets. The scrolls are linear with no fragmentation. Detail TEM showing controlled unrolling from (b) rolled, (f) to partially unrolled, and to (j) unrolled nanosheets. (c, g, k) AFM topography images, with the locations of the (d, h, i) associated cross-sectional height profiles indicated by green lines in the topographies. The AFM data is consistent with the TEM data. In addition the layer thicknesses in d, h, and i are consistent with prerolled nanosheets of Figure 1

The Au nanostructure was characterized by X-ray diffraction and X-ray photoelectron spectroscopy, confirming the phase and chemical composition (see Figures S4 and S5 in the Supporting Information). The 2D-nanosheets show a pH-responsive shape transformation, becoming nanoscrolls upon changing the pH value to 10. The nanoscrolls unroll partially at pH 5 and become fully flat 2D-nanosheets at pH 3. This transformation, from the initially flat nanosheets at pH 6 (shown previously in Figure 1e) to nanoscrolls at pH 10, partially unrolled nanoscrolls at pH 5, and back to flat nanosheets at pH 3 is shown in Figure 2a–c, 2e–g, and 2i–k, respectively. We assume that the hysteretic rolling behavior as a function of pH is caused by some plastic deformation of the nanoporous Au during rolling, particularly at the ligament areas, which must be reversed when unrolling. The nanoscrolls are uniform with straight edges, the number of turns depending on the size of the original nanosheets, and have a typical scroll thickness of 2–4 layers (Figure 2d). The nanosheets and nanoscrolls have consistent dimensions, and no fragments or residual materials were observed on the substrate, indicating that no damage occurred during the shape transformation process, as monitored by TEM (Figure 2a, e, i) and AFM topography and cross-sectional height profile as shown in Figures 2c, g, k and 2d, h, l, respectively.

The Au depositions were controlled to achieve coverage resulting in a percolating condition on the surface of the polymer. To verify the criticality of this percolating condition we performed additional experiments, consisting of preparation of samples with Au coverage well below the percolation threshold. These samples were found to be unstable, and did not form nanosheets upon exfoliation, but rather aggregated (see Figure S6 in the Supporting Information). In general, the diameter of a nanoscroll scales with the thickness of the wall and the net strain in the system. In our case, since the thickness of the 2D nanosheets is limited by the Au percolating coverage requirement, we tuned the strain by changing the molecular weight (M_w) of the polymer. When the Mw of the polymer was increased from 25 kDa to 750 kDa the diameter of the nanoscrolls increased, as shown in the TEM micrographs (see Figure S7a, b in the Supporting Information). These high Mw nanoscrolls appear relaxed when precipitated on a solid substrate as result of the increased weight of the walls. The AFM topography and cross-sectional height profile (see Figure S7c, d in the Supporting Information) show a thickness proportional to the number of turns.

The shape transformation between 1D nanoscrolls and 2D nanosheets was monitored by UV–visible spectroscopy and zeta-potential measurements. Absorbance spectra were obtained for nanosheets at several pH values. As the pH value was increased, the absorbance spectra changed from a spectrum typical of a thin film (2D nanosheet), with a flat shoulder at long wavelengths; to a spectrum typical of a metallic 1D nanostructure (nanoscroll) with a peak corresponding to the longitudinal SPR of Au and a decreasing absorbance at longer

dx.doi.org/10.1021/am5041708 | ACS Appl. Mater. Interfaces 2014, 6, 13339–13343

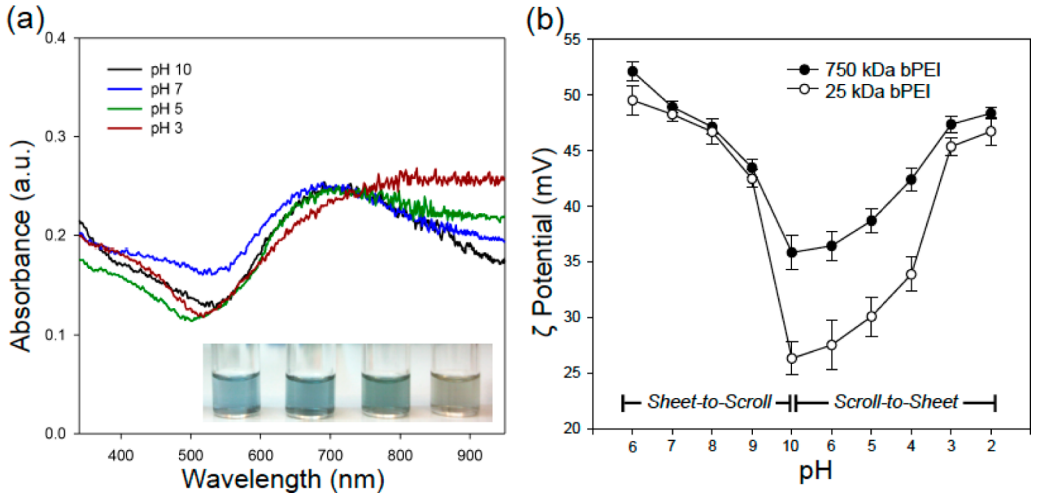

Figure 3. pH-dependent optical properties (a) Absorbance spectra of the nanosheets and nanoscrolls (25 kDa bPEI) at pH's of 3, 5, 7, and 10, showing shape transformation from flat nanosheets to nanoscrolls. The colors of nanosheet/nanoscroll dispersions are shown with pH decreasing from left to right. (b) Positive zeta-potentials are indicative of the stability of nanosheets at all protonation states, corresponding to pH's in the range 3−10.

wavelengths (Figure 3a).[19,20] Zeta-potential values corresponding to the protonation states (pH values) of two different polymers of different molecular weights were measured (Figure 3b). The positive potentials indicate that the structures are stable over a wide range of pH values from 3−10, and confirm that the polymer is strongly adsorbed onto the Au nanodomains.[21] To evaluate the transversal shape changes with pH, the well-defined zeta potential shifts of the nanosheets were observed corresponding to pH changes (see Figure S8 in the Supporting Information). These showed repeated iterations of rolling/unrolling, of up to three cycles in response to changes in pH. Yet, in the third cycle, some unstable zeta potential peak on unrolling at the third cycle showed that the nanosheets seem to be structurally deformed or aggregated by repeated rolling/unrolling. In contrast to all other 2D systems reported in the literature, including sputter deposited metal films, the rolling is not spontaneous but controllable (selective according to the pH value), and stable configurations (flat nanosheets, partially rolled nanosheets, and nanoscrolls) exist for each protonation state (pH).

Because of their large surface area, the Au-bPEI nanostructures could be used as capturing substrates for dye molecules, such as rhodamine 6G (R6G), and provide reproducible SERS signals (Figure 4). The SERS peak intensities are significantly higher from the nanoscrolls, compared to the flat nanosheets (acquired under the same conditions, detailed in the Supporting Information). This can be attributed to stronger plasmon coupling in the 1D multiwalled nanoscrolls than in the single layered nanosheets. The gaps between adjacent Au nano domains become closer upon rolling, resulting in stronger localized electromagnetic fields between the gaps.

In conclusion, incorporation of nanostructured materials into a smart polymer matrix and controlling their shape, size, and distribution can give the resultant composite enhanced properties for more controlled movements in response to external stimulus. We demonstrated the facile synthesis and efficient design of pH responsive (3−10) Au-bPEI nanosheets with perfect rolling reversibility and adaptive optical properties. The rolling is not spontaneous (as usually reported in the literature for rolling metal, polymer bilayers and metal−polymers), but is controlled; and stable configurations exist

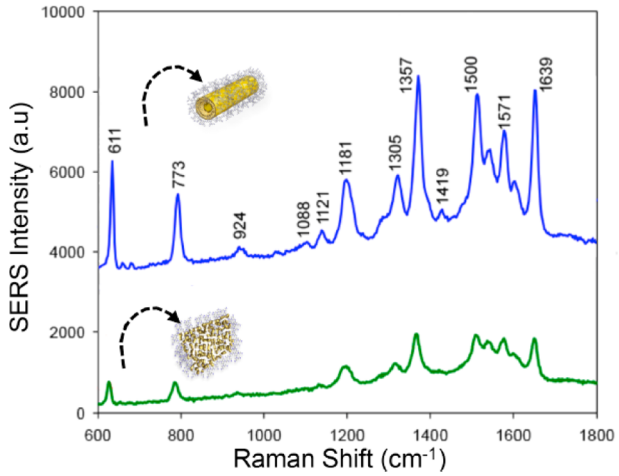

Figure 4. SERS spectra of R6G adsorbed on a nanosheet (green) and a nanoscroll (blue). The acquisition conditions and axes are identical in both cases. The SERS peak intensities are significantly higher from the nanoscrolls.

for each protonation state/pH value. The nanosheets and nanoscrolls are stable, whether free-standing or in the form of a colloidal suspension, at all pH values. They therefore appear promising for applications that require controlled and gradual two-way shape-changing materials with tremendous surface area and loading capacity. For instance, a large number of diverse nanoparticles could be loaded on the nanosheets by sputtering, followed by rolling by pH, for a customizable function. Moreover, because of their LSPR- and SERS-sensitive optical properties, nanosheet/nanoscroll colloids hold attractive potential for further applications in smart drug delivery vehicles, biosensing, catalysis, and nanotechnology contexts, from basic scientific research to commercially available products. Finally, the synthesis method is easy and general. It combines physical vapor deposition and liquid exfoliation and thus can be applied to other metals and smart polymers.

■ ASSOCIATED CONTENT

Supporting Information

Experimental details and Figure S1−S8. This material is available free of charge via the Internet at http://pubs.acs.org.

■ AUTHOR INFORMATION

Corresponding Authors

*E-mail: jeong-hwan.kim@oist.jpTel: +81-10-62334204.
*E-mail: mukhles@oist.jp.

Notes

The authors declare no competing financial interest.

■ ACKNOWLEDGMENTS

Special thanks to Dr. Chhagan Lal for XPS measurement and Mr. Antony Galea for editing the manuscript.

■ REFERENCES

(1) Sanchez, C.; Arribart, H.; Giraud-Guille, M. M. Biomimetism and Bioinspiration as Tools for the Design of Innovative Materials and Systems. *Nat. Mater.* **2005**, *4*, 277−288.

(2) Liu, K.; Tian, Y.; Jiang, L. Bio-inspired Superoleophobic and Smart Materials: Design, Fabrication, and Application. *Prog. Mater. Sci.* **2013**, *58*, 503−564.

(3) Liu, K.; Jiang, L. Bio-inspired Design of Multiscale Structures for Function Integration. *Nanotoday* **2011**, *6*, 155−175.

(4) Espinosa, H. D.; Rim, J. E.; Barthelat, F.; Buehler, M. J. Merger of Structure and Material in Nacre and Bone−Perspectives on *de novo* Biomimetic Materials. *Prog. Mater. Sci.* **2009**, *54*, 1059−1100.

(5) Finnemore, A.; Cunha, P.; Shean, T.; Vignolini, S.; Guldin, S.; Oyen, M.; Steiner, U. Biomimetic Layer-by-layer Assembly of Artificial Nacre. *Nat. Commun.* **2012**, *3*, 966−972.

(6) Martien, A.; et al. *E*merging Applications of Stimuli-responsive Polymer Materials. *Nat. Mater.* **2010**, *9*, 101−113.

(7) Lupitskyy, R.; Roiter, Y.; Tsitsilianis, C.; Minko, S. From Smart Polymer Molecules to Responsive Nanostructured Surfaces. *Langmuir* **2005**, *21*, 8591−8593.

(8) Milner, S. T. Polymer Brushes. *Science* **1991**, *251*, 905−914.

(9) Mendes, P. M. Stimuli-responsive Surfaces for Bio-applications. *Chem. Soc. Rev.* **2008**, *37*, 2512−2529.

(10) Aguilar, M. R.; Elvira, C.; Gallardo, A.; Vasquez, B.; Román, J. S. Smart Polymers and Their Applications as Biomaterials. In *Topics in Tissue Engineering*; Ashammakhi, N., Reis, R. L., Chiellini, E., Eds.; University of Oulu: Oulu, Finland, 2007; Vol. 3, pp 2−27.

(11) Kumar, A.; Srivastava, A.; Galaev, I. Y.; Mattiasson, B. Smart Polymers: Physical Forms and Bioengineering Applications. *Prog. Polym. Sci.* **2007**, *32*, 1205−1237.

(12) Meng, H.; Li, G. Reversible Switching Transitions of Stimuli-responsive Shape Changing Polymers. *J. Mater. Chem. A* **2013**, *1*, 7838−7865.

(13) Milner, S. T.; Witten, T. A.; Cates, M. E. Theory of the Grafted Polymer Brush. *Macromolecules* **1988**, *21*, 2610−2619.

(14) Milner, S. T.; Witten, T. A.; Cates, M. E. Effects of Polydispersity in the End-grafted Polymer Brush. *Macromolecules* **1989**, *22*, 853−861.

(15) Kelley, T. W.; Schorr, P. A.; Johnson, K. D.; Tirrell, M.; Frisbie, C. D. Direct Force Measurements at Polymer Brush Surfaces by Atomic Force Microscopy. *Macromolecules* **1998**, *31*, 4297−4300.

(16) Choudhury, C. K.; Roy, S. Structural and Dynamical Properties of Polyethylenimine in Explicit Water at Different Protonation States: a Molecular Dynamics Study. *Soft Matter* **2013**, *9*, 2269−2281.

(17) Schwartzkopf, M.; Buffet, A.; Körstgens, V.; Metwalli, E.; Schlage, K.; Benecke, G.; Roth, S. V.; et al. From Atoms to Layers: In Situ Gold Cluster Growth Kinetics during Sputter Deposition. *Nanoscale* **2013**, *5*, 5053−5062.

(18) Yu, X.; Duxbury, P. M.; Jeffers, G.; Dubson, M. A. Coalescence and Percolation in Thin Metal Films. *Phys. Rev. B* **1991**, *44*, 13163−13166.

(19) Siegel, J.; Lyutakov, O.; Rybka, V.; Kolská, Z.; Švorčík, V. Properties of Gold Nanostructures Sputtered on Glass. *Nanoscale Res. Lett.* **2011**, *6*, 96−104.

(20) Dixon, M. C.; Daniel, T. A.; Hieda, M.; Smilgies, D. M.; Chan, M. H.; Allara, D. L. Preparation, Structure, and Optical Properties of Nanoporous Gold Thin Films. *Langmuir* **2007**, *23*, 2414−2422.

(21) Gong, X.; Ngai, T. Interactions between Solid Surfaces with Pre-adsorbed Poly (ethylenimine) (PEI) layers: Effect of Unadsorbed Free PEI Chains. *Langmuir* **2013**, *29*, 5974−5981.